Kinetics and Catalysis, Vol. 43, No. 2, 2002, pp. 223–232. Translated from Kinetika i Kataliz, Vol. 43, No. 2, 2002, pp. 245–255.

Cluster Models of the VO_x/TiO_2 Supported Catalyst

E. P. Mikheeva, N. A. Kachurovskaya, and G. M. Zhidomirov

Boreskov Institute of Catalysis, Siberian Division, Russian Academy of Sciences, Novosibirsk, 630090 Russia

Received August 20, 2001

Abstract—Molecular structures of the active vanadium phase of the VO_x/TiO_2 supported catalyst are calculated in the framework of the cluster approximation of density functional theory (DFT). It is shown that vanadium can be stabilized on the anatase (001) surface both in the tetrahedral and octahedral coordinations with the formation of monoxo- and dioxovanadyl structures. The energy of the dioxovanadyl structure binding to the support surface is 600–800 kJ/mol. The formation of dioxovanadyl structures from monoxovanadyl ones with the formation of water molecules is energetically favorable. The effect of support on the electronic state and acidic properties of the supported vanadium phase is discussed.

INTRODUCTION

VO_x supported on TiO_2 is an important commercial catalyst for the partial oxidation of hydrocarbons [1–3], the selective reduction of NO by ammonia [4–6], and several other reactions. The catalyst with a low concentration of V_2O_5 (3–5 wt %), which is close to a monolayer, shows high activity, selectivity, and resistance to sintering and restructuring under conditions of catalytic processes. Individual oxides V_2O_5 and TiO_2 do not possess such properties [7]. The V_2O_5/TiO_2 system is a striking example of the strong interaction between a support and an active phase. The properties of the vanadium-containing active phase are determined by the support. The physicochemical and catalytic properties of the vanadium–titanium catalyst have been studied extensively for the two last decades. Analysis of the monolayer VO_x/TiO_2 catalyst using high-resolution transmission electron microscopy (HRTEM) showed that the vanadium phase has a different structure from V_2O_5. Rather, it is an amorphous surface layer. Its thickness is either 0.9–1.0 nm [8] or 1.5–2.5 nm [9]. Separate crystallites of V_2O_5 are above this layer. The molecular structure of the surface vanadium species has been studied by laser Raman spectroscopy [10, 11], ^1H and ^{51}V NMR [12–14], FTIR spectroscopy [15, 16], ESR [17], XPS [18, 19], XANES/EXAFS [20], and photoelectron diffraction [21].

Most researchers assume that the amorphous monolayer coverage of the VO_x/TiO_2 catalyst in the oxidative atmosphere consists of discrete hydroxy-, monoxo-, and dioxovanadium groups [12, 13, 22–26] in tetrahedral and octahedral coordinations. Deo and Wachs [27] also considered the formation of polyvanadates (specifically, decavanadates). Vanadium–titanium catalysts have been prepared by different methods: $VOCl_3$ deposition from the gas phase, titania impregnation by the solutions of vanadyl oxalate or ammonium vanadate, and the thermal treatment of the mechanical TiO_2–V_2O_5 mixture. After achieving the equilibrium state of the surface, the amorphous VO_x layer with similar molecular structures of vanadium species was observed on all catalysts [28].

It catches the eye that, despite numerous experimental studies devoted to the identification of the molecular structure of vanadium species, only three models [20, 29, 30] were proposed for the structural units of a monolayer in the VO_x/TiO_2 catalysts. Based on XANES/EXAFS studies, the tetrahedral coordination and the existence of two vanadyl oxygen atoms were proposed [20, 26]. Vanadium forms the other two bonds with bridging oxygen atoms of anatase. Wachs [29] proposed a simple model of the monoxide species based on laser Raman spectral data. He also assumed that vanadium is tetracoordinated and has only one vanadyl oxygen atom, whereas three bonds are taken by anatase oxygen atoms. Carlson and Griffin [30] assumed that there is a monolayer $V_2O_5(001)$ structure on the anatase (001) surface. They assigned the lattice parameters of anatase to this structure and ignored the necessity of adjusting the interface boundary between V_2O_5 and TiO_2. Based on the proposed models, Devriendt *et al.* [21] carried out single scattering cluster calculations them to the azimuthal spectra of photoelectron diffraction. These authors conclude that the best fit of calculated and experimental points is achieved for Ti_{2p}, O_{1s}, and V_{2p} peaks of the Carlson–Griffin model [30].

The geometric complementarity between the $V_2O_5(010)$ surface and $TiO_2(010)$ and $TiO_2(001)$ surfaces was considered in [31] as one of the main factors enabling the formation of the monolayer coverage of the VO_x/TiO_2 catalyst. Sayle *et al.* [32] computationally modeled the VO_x/TiO_2 interface boundary using methods of molecular mechanics (and the computer program MARVIN). They found that the best geometric complementarity is achieved between the V_2O_5 (001) and $TiO_2(001)$ surfaces. The optimization of the interface boundary between these crystalline faces is

0023-1584/02/4302-0223$27.00

achievable with smaller deformations and tension of the V_2O_5 and TiO_2 structures. The formation of the coherent $(001)V_2O_5/(001)TiO_2$ boundary is accompanied by changes in the bond lengths and angles of vanadyl oxygen atoms in V_2O_5 in the layer that is nearest to the anatase support. However, in the second and third layers above the first one, the crystalline structure of V_2O_5 remains perfect. This result contradicts experimental data according to which the structure of vanadium-containing monolayer coverage in the VO_x/TiO_2 catalyst differs from the crystalline structure of V_2O_5, and the interface boundary between the vanadium oxide and anatase is amorphous to the depth of 2–3 monolayers [8, 9].

In this work, we used the cluster method to describe the coherent interface boundary of vanadium with anatase and calculated several molecular structures that describe the interaction of the active V_2O_5 phase with the (001) anatase surface.

CALCULATION DETAILS

Calculations were carried out using the computer program ADF and density functional theory (DFT) with basis sets of types I, II, III, and IV, which differ in the number of frozen inner-core orbitals. Simplified basis I without polarization functions was used for pseudoatoms H* introduced at the cluster boundaries. For titanium and vanadium atoms, we used basis set II.2*p*, which involves the *d–z* basis series without polarization functions and frozen 1*s*, 2*s*, and 2*p* orbitals. Oxygen and nitrogen atoms were calculated with basis set III.1*s* with the frozen 1*s* orbital. This basis set differed from basis set II in that the polarization functions (*t–z* series) were present. The ammonium ion NH_4^+ and the hydroxyl groups V–OH were calculated for the hydrogen atom in basis set IV, which contained the *t–z* basis series and an additional 2*p* polarization function for hydrogen.

The fragments of regular crystalline lattices of anatase and vanadium pentoxide were chosen as cluster models of individual oxides—TiO_2 and V_2O_5. For saturating the broken bonds on the boundary of a cluster and the bulk phase, we introduced pseudoatoms H*. Initially, these pseudoatoms were placed at a distance of 1 Å from oxygen atoms in the direction of the broken oxygen–metal bonds. Then, the position of boundary pseudoatoms H* was fixed and geometry optimization of all cluster atoms was carried out.

For geometry optimization and the calculation of binding energies in cluster structures, we used the local density approximation (LDA) with the exchange-correlation Vosko–Wilk–Nusair (VWN) functional.

CLUSTER MODELS AND CALCULATION RESULTS

In this work, the (001) crystalline face of anatase was modeled by both monolayer clusters ($[Ti_3O_{11}H_9]^{-1}$ (Fig. 1a), $[Ti_4O_{12}H_8]^0$ (Fig. 1b), $[Ti_4O_{14}H_{11}]^{-1}$ (Fig. 1c)), and the two-layer cluster $[Ti_3O_{12}H_{11}]^{-1}$ (Fig. 1d), which took into account the lower layers. The (001) face was chosen because it is the most frequent (together with the (010) face) on polycrystalline anatase samples [33]. On the other hand, this face is the most complementary to the (001) and (010) faces of V_2O_5 from the geometry standpoint [31, 32]. After optimization, the lengths of Ti–O bonds in the clusters were changed within 10% in agreement with experimental data on the relaxation of the TiO_2 surface [34].

When modeling the structure of monoxovanadyl species, we took into account the following experimental facts:

(1) The interactions of vanadium-containing components with the anatase surface occur via the surface OH groups [12, 35].

(2) OH groups of two types are available on the anatase surface: with the localization of protons on bridging and terminal oxygen atoms [36, 37].

(3) Monovanadyl species have the structure of distorted tetrahedrons and contain vanadyl oxygen [29] and the OH group [12].

We calculated the molecular structure

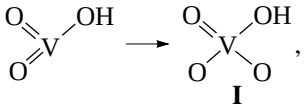

I

which corresponded to conditions (1)–(3). Optimized structure **I** on the anatase (001) surface is shown in Fig. 2a. Vanadium is bound to the terminal and bridging oxygen atoms of anatase. The bond lengths are l(V=O) = 1.600 Å, l(V–OH) = 1.810 Å, $l(V–O_{term})$ = 1.725 Å, and $l(V–O_{bridging})$ = 1.847 Å. The energy of the oxovanadyl structure binding to the support was calculated using the formula

$$E_b = E_{VO_x/TiO_2} - (E_{VO_x} + E_{TiO_2}), \quad (1)$$

where E_{VO_x/TiO_2}, E_{VO_x}, and E_{TiO_2} are the total energies of the TiO_2 binding to the supported VO_x structure, VO_x, and the TiO_2 support, respectively. In the case of monoxovanadyl structures of initial VO_x, we took the structure 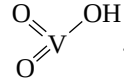 . The binding energies of two monoxovanadyl structures (Fig. 2a) with support was E_b = –289.9 kJ/mol.

The authors of [22, 26] assume that, in addition to monovanadyl species, polymerized structures with one or two bridging oxygen atoms are present on the surface of the monolayer VO_x/TiO_2 catalyst. Dioxova-

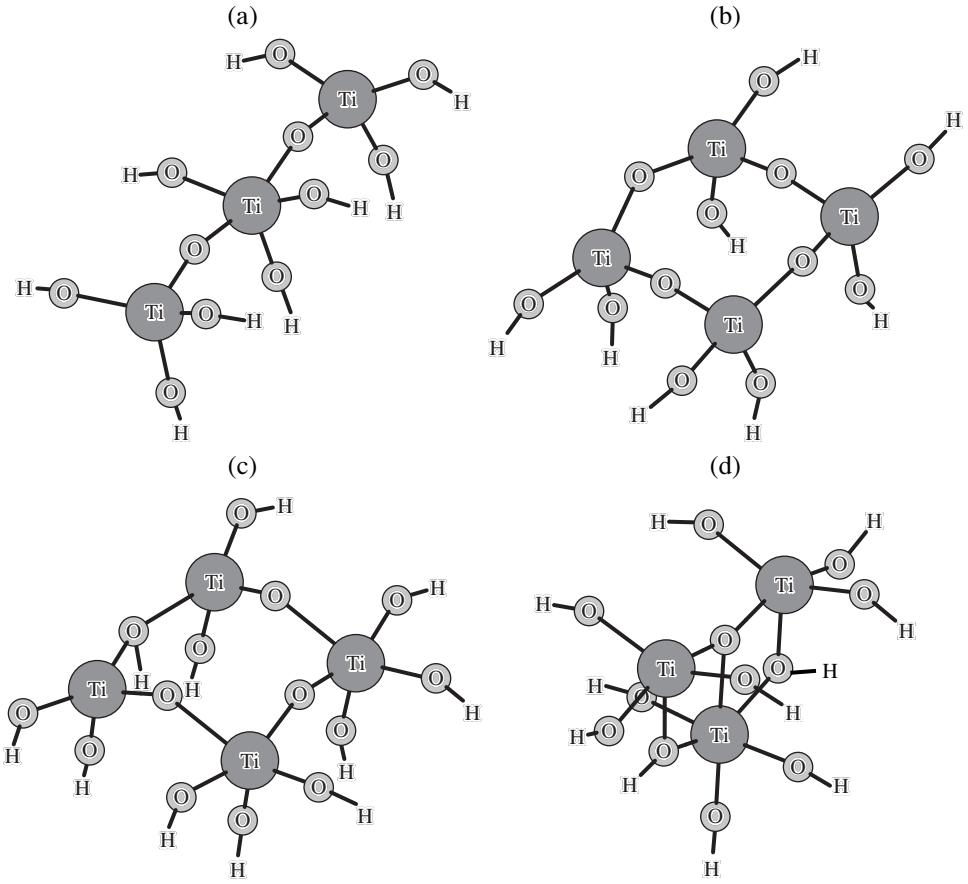

Fig. 1. Cluster models of the anatase (001) surface: (a) cluster $[Ti_3O_{11}H_9]^{-1}$, (b) cluster $[Ti_4O_{12}H_8]^0$, (c) cluster $[Ti_4O_{14}H_{11}]^{-1}$, and (d) cluster $[Ti_3O_{12}H_{11}]^{-1}$.

nadyl species with tetrahedral and octahedral envelopes of vanadium ions are considered in [24–26]. The following structures were proposed:

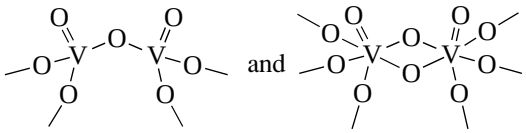

II **III**

According to our calculations, structures **II** and **III** can be obtained by covering the anatase surface with the molecular species

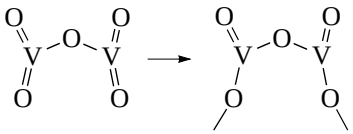

IV

Structure **IV** was chosen for the following reasons:

(1) Vanadium and oxygen in **IV** are in the stoichiometric ratio, and this structure has no charge.

(2) The crystalline phase of vanadium pentoxide can be described (Fig. 3a) as a set of chains consisting of structures **IV**. The way in which they connect to each other determines the crystalline structure V_2O_5, and the structures **IV** determine the short-range interactions in vanadium pentoxide. In amorphous structures, short-range interactions are usually preserved.

Structure **II** was obtained by layering **IV** on the $[Ti_3O_{12}H_{11}]^{-1}$ cluster (Fig. 2b) so that two vanadyl oxygen atoms formed bonds with two adjacent titanium ions along the [100] direction. The [100] direction on the anatase surface was chosen on the basis of geometrical complementarity: the positions of oxygen atoms along the [100] directions on the V_2O_5 and TiO_2 surfaces virtually coincide. After carrying out optimization, one more V–O bond is formed with the bridging TiO_2 oxygen atom and the vanadium ion becomes tetracoordinated (Fig. 2b) with the following bond lengths: l(V=O) = 1.606 Å, l(V–O–V) = 1.788 Å, l(V–O_{term}) = 1.697 Å, and l(V–$O_{bridging, Ti}$) = 1.794 Å.

To estimate the effect of choosing the support model on the geometry and energy of vanadyl structure binding to the anatase (001) surface, structure **IV** was layered on clusters $[Ti_4O_{12}H_8]^0$, $[Ti_4O_{14}H_{11}]^{-1}$, and $[Ti_3O_{12}H_{12}]^0$ in addition to cluster $[Ti_3O_{12}H_{11}]^{-1}$. The

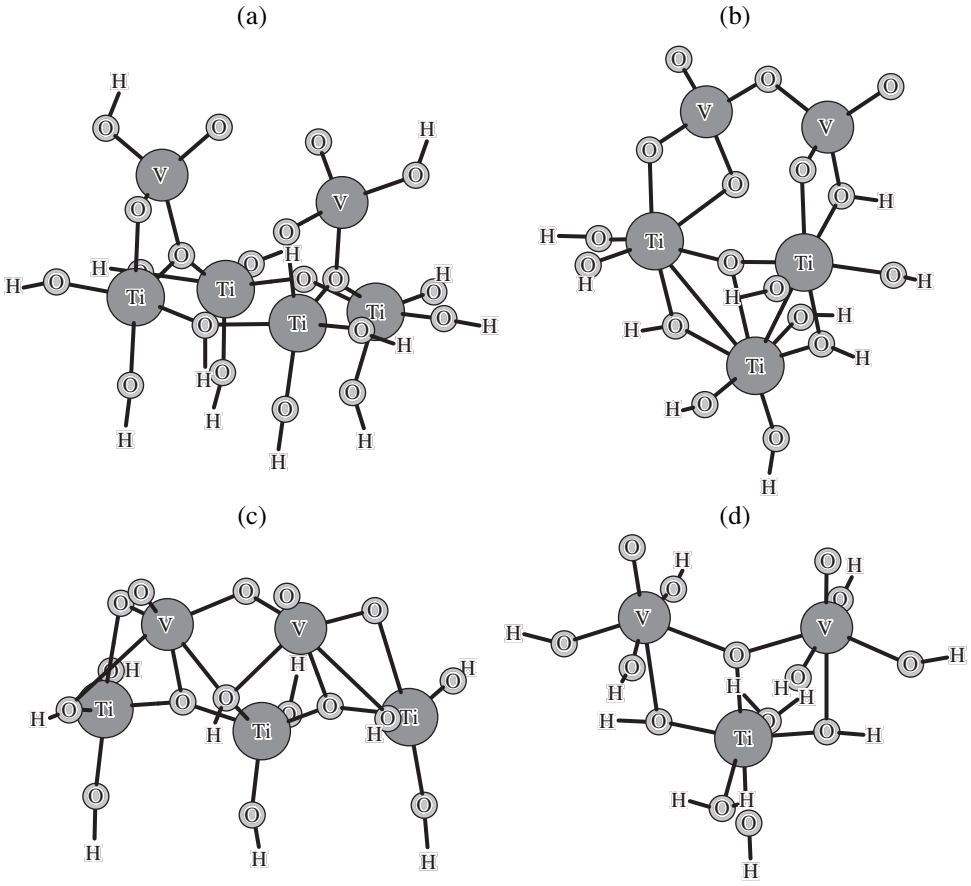

Fig. 2. Cluster models of the VO_x/TiO_2 catalyst: (a) cluster $[V_2O_6H_2/Ti_4O_{14}H_{11}]^{-1}$, monoxovanadyl structures **I** on the anatase surface; (b) cluster $[V_2O_5/Ti_3O_{12}H_{11}]^{-1}$, dioxovanadyl structure **II** with one bridging oxygen; (c) cluster $[V_2O_5/Ti_3O_{11}H_9]^{-1}$, dioxovanadyl structure **III** with two bridging oxygens on the anatase (001) surface; and (d) cluster $[TiV_2O_{14}H_{13}]^{-1}$, the model with two V^{x+} embedded in the anatase lattice.

results of calculations are shown in Table 1. The energies of dioxovanadyl binding to the support were calculated by formula (1). The structure of the V_2O_5 molecule was chosen to begin calculations. As can be seen from Table 1, the energy of molecular vanadyl binding to the support changes substantially if the second layer of the crystalline lattice in the cluster model of the support is taken into account. For the $[VO_x/Ti_4O_{18}H_8]^{-1}$ model, E_b = –139.83 kJ/mol, although for the two-layer cluster $[VO_x/Ti_3O_{12}H_4]^{-1}$ E_b is –870.42 kJ/mol. When a deeper layer is considered in the planar model by introducing the proton bound to the bridging oxygen atom Ti–O(H)–Ti on the [100] axis, along which structure **IV** is layered, the binding energy E_b increases to –600 kJ/mol. According to the results shown in Table 1, the choice of the cluster model of support weakly affects the lengths of bonds between vanadium and vanadyl V=O or bridging V–O–V oxygen atoms. They change within 0.01–0.02 Å, although the lengths of two other bonds of vanadium with the bridging oxygen of Ti ($V–O_{Ti}$) and bridging oxygen V–O–Ti with Ti increase to 0.1–0.15 Å for the planar model of support $[Ti_4O_{12}H_8]^0$.

Structural model **III** with two bridging oxygen atoms between vanadium atoms and with the octahedral oxygen environment of vanadium ions was obtained by coordinating structure **IV** to the $[Ti_3O_{11}H_9]^{-1}$ cluster. Two vanadyl oxygen atoms of structure **IV** were bound to two terminal titanium ions of the $[Ti_3O_{11}H_9]^{-1}$ cluster, and the bridging oxygen atom V–O–V was bound to the central titanium ion. After optimization, the geometry of the surface species changed so that each vanadium atom formed two bonds with two bridging oxygen atoms of anatase and one bond with the central bridging oxygen (Fig. 2c). Vanadium became six-coordinated and the bond lengths were l_1 = 1.609 Å for vanadyl oxygen V=O, l_2 = 1.819 Å and l_3 = 2.129 Å for two bridging oxygen atoms V(O)(O)V, l_4 = 2.250 Å and l_5 = 2.394 Å for bridging oxy-

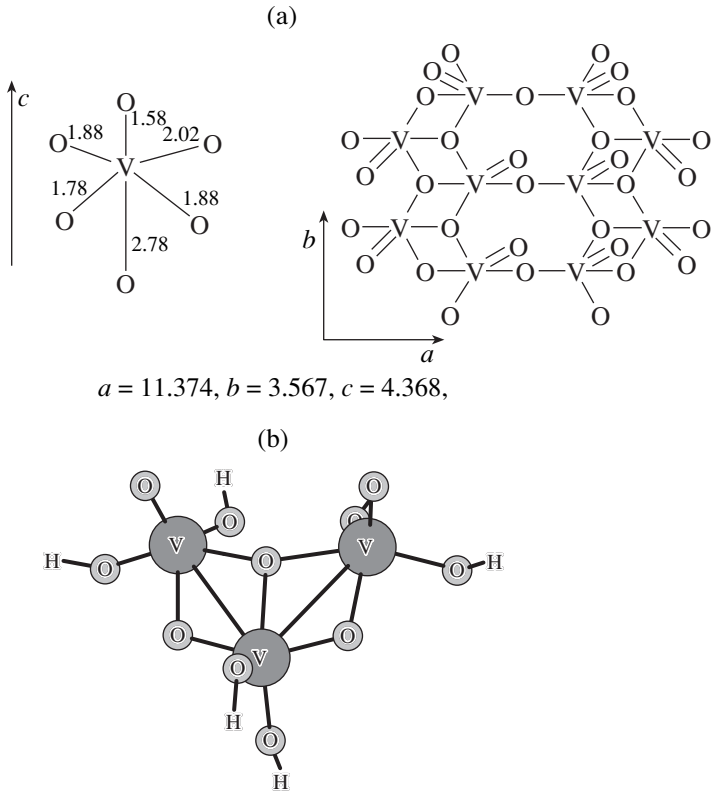

Fig. 3. (a) Crystalline structure of vanadium pentoxide and (b) cluster $[V_3O_{11}H_6]^{-1}$, a model of the $V_2O_5(001)$ surface. Bond lengths are in angstroms.

gen atoms of the lattice, and $l_6 = 1.679$ Å for V–O of the bridging oxygen atom $V^{-O-}Ti$. The energy of structure **IV** binding to anatase (cluster $[V_2O_5/Ti_3O_{11}H_9]^{-1}$) is –600 kJ/mol.

In our earlier paper [38], we considered the cluster models of six-coordinated vanadium incorporated in the anatase lattice by the isomorphic substitution of titanium ions for vanadium ions. Electric conductivity measurements in the process of vanadium ion deposition and in the process of nitrogen oxide reduction by ammonia [39, 40] suggested the possibility of vanadium dissolution in the upper layers of support. In this work, we return to the model (Fig. 2d) of vanadium embedded into a TiO_2 matrix to compare the acidic properties of this structure with the properties of the vanadium phase supported on TiO_2.

In this work, we only considered the Brønsted acid sites V–OH, which are the sites for ammonia adsorption. According to IR data [41, 42], they are present on both the V_2O_5 and VO_x/TiO_2 catalysts.

We calculated the ammonium ion in ammonia adsorption on the binuclear V(OH)–O–V(O) site, which was present in the structures used as cluster models:

(1) Vanadium embedded in the anatase lattice (cluster $[H/TiV_2O_{14}H_{13}]^0$);

(2) Vanadium supported on the $TiO_2(001)$ surface with one bridging oxygen $V^{-O-}V$ (cluster $[H/V_2O_5/Ti_3O_{12}H_{11}]^0$);

(3) Vanadium supported on the $TiO_2(001)$ surface with two bridging oxygen atoms $V\begin{smallmatrix}O\\O\end{smallmatrix}V$ (cluster $[H/V_2O_5/Ti_3O_{11}H_9]^0$);

(4) Unsupported V_2O_5 (cluster $[H/V_3O_{11}H_6]^-$); the fragment of the (001) surface of vanadium pentoxide is described by the $[V_3O_{11}H_6]^-$ cluster (Fig. 3b).

Ammonia protonation with the formation of the ammonium ion is observed for all structures except structure (3) (cluster $[H/V_2O_5/Ti_3O_{11}H_9]^0$).

For structure (3), the ammonium ion is formed in the optimization process as a transition state. After optimization, ammonium is bound by the strong hydrogen bond with one V–OH site. For other structures, the ammonium ion is formed from adsorbed ammonia in the optimization process equally readily on both symmetric clusters (with symmetries C_{2V} and C_s) and when the symmetry is decreased to C_1. This was used as a criterion for the achievement of the local minimum on the potential energy surface in ammonia adsorption on the clusters $NH_4/TiV_2O_{14}H_{13}$ (Fig. 4a), $NH_4/V_2O_5/Ti_3O_{12}H_{11}$ (Fig. 4b), and $NH_4/V_3O_{11}H_6$

(Fig. 4c). The results of calculation are summarized in Tables 2 and 3.

As follows from Table 3, we observe for the above clusters relatively small changes in the energy of NH_4^+ stabilization: E_{NH_3} for model (1) (cluster $NH_4/TiV_2O_{14}H_{13}$) is 20.5 kJ/mol higher than for the crystalline unsupported V_2O_5 (model (4), cluster $NH_4/V_3O_{11}H_6$); E_{NH_3} for model (2) (cluster $NH_4/V_2O_5/Ti_3O_{12}H_{11}$) is 27.1 kJ/mol lower than for model (4). The calculated energies of NH_4^+ stabilization do not contradict experimental thermal desorption data: the activation energy of ammonia thermal desorption is 18–26 kcal/mol for V_2O_5 [42] and 22–28 kcal/mol for the supported VO_x/TiO_2 catalyst [4].

We also calculated the energy of deprotonation for the clusters $H/TiV_2O_{14}H_{13}$, $H/V_2O_5/Ti_3O_{12}H_{11}$, and $H/V_3O_{11}H_6$. The resulting data are presented in Table 3. The energy of ammonium stabilization increases in inverse proportion to the energy of proton abstraction from a cluster. Therefore, we conclude that the deprotonation energy in these mixed oxide systems is a poor acidity index for the active sites in zeolites.

DISCUSSION

This work is the first attempt to use quantum-chemical calculations in the studies of molecular structure of the monolayer VO_x/TiO_2 catalyst. The results of calculation agree with available experimental data on the possibility of vanadium stabilization on the TiO_2 (001) surface both in tetrahedral and octahedral coordinations with respect to oxygen. The localization of the mono- and dioxovanadyl structures **I**, **II**, and **III** on the TiO_2 (001) surface is energetically favorable. The energies of structures **II** and **III** are about the same (600–800 kJ/mol). There are no data on the V–O bond lengths for oxovanadyl structures. Only one work is known [26] where the bond lengths were estimated for the tetrahedral monovanadyl structure based on XANES/EXAFS spectra. The authors of that work assume that structure **I** has two vanadyl oxygen atoms with a V=O bond length of 1.65 Å and two bonds with bridging oxygen atoms of anatase (1.90 Å). However, IR spectroscopic data [15] and kinetic data on oxygen isotope exchange [43] suggest that monovanadyl structure has only one vanadyl oxygen. According to our calculation, the bond lengths in structure **I** are $l(V{=}O)$ = 1.600 Å for vanadyl oxygen, $l(V–O)_{term}$ = 1.725 Å for

Table 1. Energies and bond lengths of monoxo- and dioxovanadyl molecular structures on the anatase surface

Structure	Cluster	Binding energy, kJ/mol	Bond length, Å			
			V=O	V–O–V	V–O–Ti	V–$O_{bridging, Ti}$
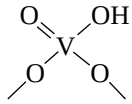	$[V_2O_6H_2/Ti_4O_{14}H_{11}]^{-1}$ (Fig. 2a)	–289.90	1.600	V–OH 1.810	V–O 1.725 O–Ti 2.014	1.847
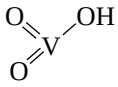	VO_2OH	–3499.71	–	–	–	–
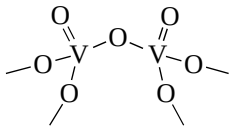	$[V_2O_5/Ti_4O_{12}H_8]^0$	–139.83	1.612	1.780	V–O 1.677 O–Ti 2.132	1.899
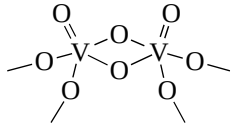	$[V_2O_5/Ti_4O_{14}H_{11}]^{-1}$	–606.38	1.611	1.789	V–O 1.716 O–Ti 2.003	1.836
	$[V_2O_5/Ti_3O_{12}H_{11}]^{-1}$ (Fig. 2b)	–870.42	1.606	1.788	V–O 1.697 O–Ti 1.985	1.794
	$[V_2O_5/Ti_3O_{12}H_{12}]^0$	–830.54	1.590	1.779	V–O 1.711 O–Ti 1.975	1.804
	$[V_2O_5/Ti_3O_{11}H_9]^{-1}$ (Fig. 2c)	–600.03	1.609	l_2 = 1.819 l_3 = 2.129	V–O 1.679 O–Ti 2.324	l_4 = 2.250 l_5 = 2.394
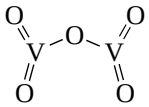	V_2O_5	–5366.46	–	–	–	–

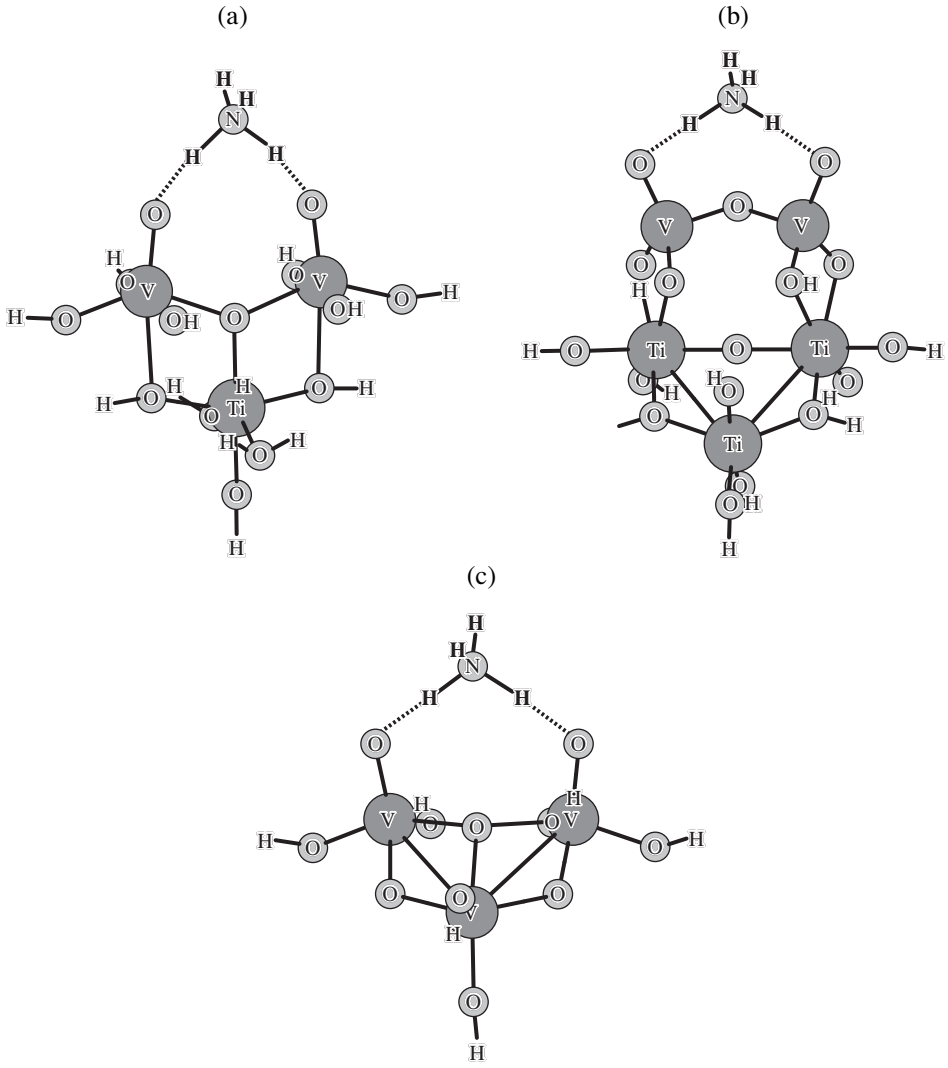

Fig. 4. Ammonia adsorbed on (a) cluster $[H/TiV_2O_{14}H_{13}]^0$ with two V^{x+} embedded in the anatase lattice; (b) cluster $[H/V_2O_5/Ti_3O_{12}H_{11}]^0$ with the dioxovanadyl structure supported on the anatase surface; and (c) cluster $H/V_3O_{11}H_6$, a model of the $V_2O_5(001)$ surface.

bridging $V\!<\!^{O}_{Ti}$, and l(V–OH) = 1.810 Å, and l(V–$O_{bridging}$) = 1.847 Å for vanadium with the OH group (V–OH) and anatase oxygen (V–$O_{bridging}$).

Quantum chemical calculations led us to conclude that dioxovanadyl structures can be formed from two monoxovanadyls (with water formation) according to the reaction

$$2\ \mathrm{O{=}V(OH)(O)(O)} \longrightarrow \mathrm{O{=}V(O)(O)\text{-}O\text{-}V(O)(O){=}O} + H_2O, \qquad (I)$$

which occurs with a gain in energy equal to 115.1 kJ/mol. When water molecules transform into the adsorbed state, this gain is even more pronounced.

The study of monolayer VO_x coverage of TiO_2 by spectroscopic methods showed that the structure and charge of surface vanadyl species rapidly changes with a change in the redox medium and moistness. Based on diffuse-reflectance spectra, Carcfa *et al.* [44] concluded that the number of isolated vanadyl groups in the VO_x/SiO_2 samples depends on the extent of surface hydration. According to our calculations, the dehydration of the VO_x/TiO_2 catalysts should switch the equilibrium of reaction (I) toward the formation of dioxovanadyl species.

It is interesting to compare the energetic characteristics of structures **II** and **III** considered in this work with a change in the interface energy when the monolayer coverage $V_2O_5(001)/TiO_2(001)$ is formed. Sayle *et al.* [32] noted that the best geometric complementarity exists between these surfaces enabling the possibility for the formation of a chemical bond between vanadyl oxygen atoms of the V_2O_5 monolayer that turn to the anatase surface and titanium cations. The optimization of the monolayer coverage $V_2O_5(001)/TiO_2(001)$

results in an energy gain of 0.46 J/m^2. The binding energy of structures **II** and **III** with the anatase surface is 600 kJ/mol. Taking into account that the surface area covered by structures **I** and **II** is 20 Å^2 and that the coverage of TiO_2(001) by dioxovanadyl molecular structures is monolayer, the binding energy is 5 J/m^2 in our case. This is an order of magnitude higher than the binding energy estimated using the force filed method.

In the cluster models considered above, vanadyl oxygen is also bound to titanium cations along the [100] axis of anatase. However, in the optimization process, a rather short bond is formed between the bridging oxygen atom of anatase $l(V–O_{bridging,\ Ti})$ = 1.800–1.900 Å and molecular structure **IV** becomes inclined to the (001) surface of anatase. The angle between axis *c* of anatase and the vanadyl structure is 24°–27°.

Krikova *et al.* [45] managed to detect the coherent boundary of splicing the crystalline phases of TiO_2 and V_2O_5 when 20 wt % of vanadium pentoxide is supported. The unit cells of TiO_2 and V_2O_5 are in contact so that the [100] direction is common to both phases and the angle between axes *c* is 17.4°. Apparently, it is incorrect to compare the results obtained at the level of a molecular model with crystallographic data, but the general trend is seen.

We considered various explanations for the nature of the strong interaction between the support and the supported vanadium phase.

The first explanation was proposed in [31, 45]. The authors of these papers noticed that the structural complementarity of crystalline faces of the TiO_2 support and the V_2O_5 phase should result in the strong interatomic interaction at the boundary of contacting materials. As a consequence, elastic stress appears in the crystalline lattice of anatase and causes the formation of dislocations and vacancies, some of which can be substituted by vanadium ions. Molecular cluster models obtained by the isomorphic substitution of the surface titanium ions for vanadium ions were considered in [38] and in this work.

The other explanation is based on the experimental fact that hydroxyl groups on the anatase surface participate in the formation of a chemical bond between VO_x and the support surface [35]. Molecular structures that are the structural units of the monolayer VO_x/TiO_2 catalyst were characterized by various spectroscopic methods. In this work, we carried out the quantum-

Table 2. Charges of vanadium and oxygen ions and the HOMO and LUMO energies for clusters that model unsupported V_2O_5, V^{x+} embedded in the anatase lattice, and V_2O_5 supported on the anatase surface

System	Cluster	q_V	q_O vanadyl	q_O bridging V–O–V	q_O bridging V–O–Ti	E_{HOMO}, E_{LUMO}, eV
Unsupported V_2O_5	$[V_3O_{11}H_6]^{-1}$	1.9386	–0.7072	–0.8338	–	–2.8998 –0.2150
V^{x+} embedded in the anatase lattice	$[TiV_2O_{14}H_{13}]^{-1}$	1.8294	–0.6546	–0.7697	–	–1.6650 –0.2410
Supported V_2O_5 with one bridging oxygen	$[V_2O_5/Ti_3O_{12}H_{11}]^{-1}$	1.9841	–0.7310	–0.9195	–0.7310	–3.2550 –0.6170
Supported V_2O_5 with two bridging oxygens	$[V_2O_5/Ti_3O_{11}H_9]^{-1}$	1.7157	–0.6972	–0.8503 –0.8588	–0.7653	–2.7540 –1.3460

Table 3. Charges, bond lengths, and the energies of ammonia adsorption E_{ads} and deprotonation E_{deprot}

Parameter	$H/V_3O_{11}H_6 + NH_3$	$H/TiV_2O_{14}H_{13} + NH_3$	$H/V_2O_5/Ti_3O_{12}H_{11} + NH_3$
q_V	2.0340	1.9071	2.0344
q_O	–0.7951	–0.7532	–0.8095
$q_{H(O)}$	0.3148	0.3017	0.3045
$q_{H(N)}$	0.2840	0.2749	0.3264
q_N	–0.4775	–0.4756	–0.4902
$q(NH_4)^{x+}$	0.7201	0.6678	0.7716
l(N–H(O))	1.022	1.025	1.025
l(O–H)	1.543	1.572	1.610
E_{ads}, kJ/mol	–129.74	–150.28	–102.66
E_{deprot}, kJ/mol	–79.85	–118.45	–34.83

mechanical calculation of cluster models for monoxo- and dioxovanadyl structures and showed their thermal stability on the anatase surface.

Tables 1 and 2 show the results of calculating the V–O bond lengths and charges of vanadium and oxygen ions. These results (Figs. 2a–2c and Table 1) suggest that the structural parameters (namely, the number and lengths of V–O bonds of the oxygen environment closest to V^{x+}) of the cluster models of VO_x supported on the anatase surface and V^{x+} embedded in the TiO_2 lattice differ from those for the cluster model of vanadium pentoxide.

It is well known that changes in the structural parameters lead to changes in the electronic state of the system. Table 2 shows the values of Mulliken charges for vanadium and oxygen calculated for the cluster models of V^{x+} embedded in the anatase lattice (Fig. 2d) and supported on the VO_x/TiO_2 surface (Fig. 2b). These are compared with the supported V_2O_5 (the cluster model, Fig. 3b). As can be seen from Table 2, these structures differ in the extent of the ionic character of the V–O bond, which can be defined as the ratio of the cation effective charge to the anion charge. The bond between V^{x+} embedded in the anatase lattice and oxygen is the least ionic. The bond between vanadium supported on the TiO_2 surface and oxygen is the most ionic. Unsupported vanadia forms a bond with an intermediate ionic character.

There are a lot of papers devoted to the effect of the ionic character of the metal–oxygen bond on the acidic properties of oxides. It is known that alkali metal oxides with the high ionic character have basic properties. The acidity of an oxide system also increases with an increase in the extent of covalence of a metal–oxygen bond. Pronounced Lewis and Brønsted sites were found on WO_3 and V_2O_5, which have low charges of cations and anions (compared to the maximum possible charges).

Results obtained in this work agree with the general trend toward an increase in the acidity with a decrease in the ionic character of bonds. The highest adsorption energy of ammonia E_{NH_3} = –150.28 kJ/mol was obtained for the model of V^{x+} embedded in the anatase lattice with the ionic character μ_V = 1.8294/5.0 = 0.3658. The smaller value E_{NH_3} = –129.74 kJ/mol was obtained for unsupported V_2O_5 with μ_V = 1.9386/5.0 = 0.3877. The lowest value E_{NH_3} = –102.66 kJ/mol was obtained for the model of VO_x supported on the anatase surface with μ_V = 1.9841/5.0 = 0.3968.

It was assumed in several papers [46–48] that NO oxidation by ammonia occurs between adsorbed ammonia and gas-phase NO molecules. The necessary step for this reaction is the activation of ammonia in its adsorption on the binuclear V(O)–V(OH) site with the formation of NH_4^+. However, according to our calculation, the values of the stabilization energies of ammonium ions on such a site for unsupported V_2O_5 and models of VO_x/TiO_2 catalyst are only ~20 kJ/mol. It is reasonable to consider other mechanisms for ammonia activation, specifically those associated with dissociative adsorption [49–51].

ACKNOWLEDGMENTS

This work was supported by INTAS grant no. IR-97-0059 and the Russian Foundation for Basic Research (project no. 00-15-97441).

REFERENCES

1. Wachs, I.E. and Weckhuysen, B.M., *Appl. Catal.*, 1997, vol. 157, no. 1, p. 67.
2. Centi, G., *Appl. Catal.*, 1996, vol. 147, no. 2, p. 267.
3. Narayana, K.V., Venugopal, A., and Rao, P.K., *Appl. Catal.*, 1997, vol. 150, no. 2, p. 269.
4. Efstathiou, A.M. and Fliatoura, K., *Appl. Catal. B*, 1995, vol. 6, no. 1, p. 35.
5. Georgiadov, I., Papadopoulou, C.U., Matralis, H.K., Voyiatzis, G.A., and Lycourghitis, A., Kordulisch, Ch., *J. Phys. Chem.*, 1998, vol. 102, no. 43, p. 8459.
6. Busca, G., Lietti, L., Ramis, G., and Berti, F., *Appl. Catal., B*, 1998, vol. 18, nos. 1–2, p. 1.
7. *Catal. Today*, 1994, vol. 20, no. 1.
8. Vedrine, J.C., *Catal. Today*, 2000, vol. 56, no. 4, p. 455.
9. Sanati, M., Wallenberg, L.R., Anderson, A., Jansen, S., and Tu, Y., *J. Catal.*, 1991, vol. 132, no. 1, p. 128.
10. Wachs, I.E., *Catal. Today*, 1996, vol. 27, nos. 3–4, p. 437.
11. Went, G., Oyama, S.T., and Bell, A.T., *J. Phys. Chem.*, 1990, vol. 94, no. 10, p. 4240.
12. Pinaeva, L.G., Lapina, O.B., Mastikhin, V.M., Nosov, A.V., and Balzhinimaev, B.S., *J. Mol. Catal.*, 1994, vol. 88, no. 3, p. 311.
13. Eckert, H. and Wachs, I.E., *J. Phys. Chem.*, 1989, vol. 93, no. 18, p. 6796.
14. Shubin, A.A., Lapina, O.B., and Courcot, D., *Catal. Today*, 2000, vol. 56, no. 4, p. 379.
15. Davydov, A.A., *Kinet. Katal.*, 1993, vol. 34, no. 6, p. 1056.
16. Busca, G., *Langmuir*, 1986, vol. 2, no. 5, p. 577.
17. Paganini, M.C., Acqua, L.D., Giamello, E., Lietti, L., Forzatti, P., and Busca, G., *J. Catal.*, 1997, vol. 166, no. 2, p. 195.
18. Liu, Z.X., Lin, Zh.Da., Fan, H.G., and Li, F.H., *Appl. Phys.*, 1988, vol. 45, no. 2, p. 159.
19. Bukhtiajarov, V.J., *Catal. Today*, 2000, vol. 56, no. 4, p. 403.
20. Kozlowski, R., Pettifer, R.F., and Thomas, J.M., *J. Phys. Chem.*, 1983, vol. 87, no. 25, p. 5176.
21. Devriendt, K., Poelman, H., and Fiermans, L., *Surf. Interface Anal.*, 2000, vol. 29, no. 2, p. 139.
22. Bond, G.C., Flamerz, S., and Shukri, R., *Faraday Discuss.*, 1989, vol. 87, no. 1, p. 65.
23. Bond, G.C., Zurita, J.P., and Flamerz, S., *Appl. Catal.*, 1986, vol. 27, no. 2, p. 353.

24. Wachs, J.E., Saleh, R.Y., Chan, S.S., and Cherich, C.C., *Appl. Catal.*, 1985, vol. 15, no. 2, p. 339.
25. Christiany, C., Forzatti, P., and Busca, G., *J. Catal.*, 1989, vol. 116, no. 2, p. 586.
26. Haber, J., Kozlowska, A., and Kozlowski, R., *J. Catal.*, 1986, vol. 102, no. 1, p. 52.
27. Deo, G. and Wachs, I.E., *J. Phys. Chem.*, 1991, vol. 95, no. 15, p. 5889.
28. Machej, T., Haber, J., Turek, A.M., and Wachs, I.E., *Appl. Catal.*, 1991, vol. 70, no. 1, p. 115.
29. Wachs, I.E., *Chem. Eng. Sci.*, 1990, vol. 45, no. 8, p. 2561.
30. Carlson, T. and Griffin, G.L., *J. Phys. Chem.*, 1986, vol. 90, no. 22, p. 5896.
31. Vejux, A. and Courtine, P., *J. Solid State Chem.*, 1978, vol. 23, no. 1, p. 93.
32. Sayle, D.C., Catlow, C.R.A., Perrin, M.-A., and Nortier, P., *J. Phys. Chem.*, 1996, vol. 100, no. 21, p. 8940.
33. Boehm, H.P., *Adv. Catal.*, 1996, vol. 16, p. 179.
34. Charlton, G., Howes, P.B., Nicklin, C.L., Steadman, P., Taylor, J.S.G., Muryn, C.A., Harte, S.P., Mercer, J., McGrath, R., Norman, D., Turner, T.S., and Thornton, G., *Phys. Rev. Lett.*, 1997, vol. 78, no. 3, p. 495.
35. Bond, G.C., *Appl. Catal.*, 1997, vol. 157, no. 1, p. 91.
36. Busca, G., Saussey, H., Saur, O., Lavalley, J.C., and Lorenzelli, V., *Appl. Catal.*, 1985, vol. 14, no. 2, p. 245.
37. Tret'yakov, N.E. and Filimonov, V.M., *Kinet. Katal.*, 1972, vol. 13, no. 3, p. 815.
38. Kachurovskaya, N.A., Mikheeva, E.P., and Zhidomirov, G.M., *J. Mol. Catal. A*, 2002, vol. 178, nos. 1–2, p. 191.
39. Herrmann, J.-M., *Catal. Today*, 1994, vol. 20, no. 1, p. 135.
40. Herrmann, J.-M. and Disdier, J., *Catal. Today*, 2000, vol. 56, no. 4, p. 389.
41. Ramis, G., Busca, G., and Li, Y., *Catal. Today*, 1996, vol. 28, no. 4, p. 373.
42. Srnak, T.Z., Dumesic, G.A., Clausen, B.S., Tornaquist, E., and Topsøe, N.-Y., *J. Catal.*, 1991, vol. 135, no. 1, p. 186.
43. Wachs, I.E., Deo, G., Weckhuyssen, B.M., Andreini, A., Vuurman, M.A., De Boer, M., and Amiridis, M.D., *J. Catal.*, 1996, vol. 161, no. 1, p. 211.
44. Carcfa, H., Nieto, J.M.L., Palomares, E., and Solsona, B., *Catal. Lett.*, 2000, vol. 69, nos. 3–4, p. 217.
45. Krikova, G.N., Klenov, D.O., and Zenkovets, G.A., *React. Kinet. Catal. Lett.*, 1997, vol. 60, no. 1, p. 179.
46. Topsøe, N.-Y., Topsøe, H., and Dumesic, J., *J. Catal.*, 1995, vol. 151, no. 1, p. 226.
47. Topsøe, N.-Y., Topsøe, H., and Dumesic, J., *J. Catal.*, 1995, vol. 151, no. 1, p. 241.
48. Inomata, M., Miamoto, A., and Murakami, Y., *J. Catal.*, 1980, vol. 62, no. 1, p. 140.
49. Janssen, F., van den Kerkhof, F., Bosch, H., and Ross, J.J., *Phys. Chem.*, 1987, vol. 91, no. 27, p. 6633.
50. Ramis, G., Busca, G., Bregani, F., and Forzatti, P., *Appl. Catal.*, 1990, vol. 64, nos. 1–2, p. 259.
51. Pinaeva, L.G., Sukhnev, A.P., Budneva, A.A., Paukshtis, E.A., and Balzhinimaev, B.S., *J. Mol. Catal.*, 1996, vol. 112, no. 1, p. 115.